Available online at www.sciencedirect.com
ScienceDirect
C. R. Chimie 11 (2008) 506–514
COMPTES RENDUS CHIMIE
http://france.elsevier.com/direct/CRAS2C/

Full paper / Mémoire

Measurement of short NMR relaxation times: Effect of radio-frequency pulse length

Benjamin Nicot [a,b], Marc Fleury [a,*], Jacques Leblond [b]

[a] *IFP, Département Pétrophysique, 1, avenue de-Bois-Préau, 92852 Rueil-Malmaison cedex, France*
[b] *ESPCI, Laboratoire de Physique Thermique, Paris, France*

Received 7 May 2007; accepted after revision 6 November 2007
Available online 27 December 2007

Abstract

In certain situations, such as in viscous liquids or nano-porous media, the transversal relaxation time T_2 may become so short that the pulse duration or the detector dead time is no longer negligible. These cases raise fundamental questions about relaxation during the radio-frequency pulses used in classical CPMG or Inversion-Recovery sequences. For an ideal system having a single relaxation time, we examine the effect of the finite pulse duration on the magnetization decay after the pulses occurring in FID, CPMG and Inversion-Recovery sequences. We solved analytically the Bloch equations during and after the pulses and compared the theoretical predictions with experimental data. Finally, we propose approximate simple expressions to correct the sequences for the magnetization attenuation during the pulses. IR curves are affected by transversal relaxation during the pulses, yielding asymmetric curves even if T_1 is very large. The magnetization decay obtained during a CPMG sequence is not affected by relaxation during the pulses. This is valid provided the time origin is chosen in the middle of the first pulse. ***To cite this article: B. Nicot et al., C. R. Chimie 11 (2008).***

Keywords: NMR; Relaxation; CPMG; Inversion-Recovery

1. Introduction

NMR relaxation time measurements on liquids performed at moderate or low field provide useful information about molecular dynamics. For example, viscosity can be deduced from transversal relaxation time over a very wide range of values spanning several decades. In porous media, a pore size information can be obtained from transversal and longitudinal relaxation times. In most situations, the transversal and longitudinal relaxation times are much larger than the radio-frequency (r.f.) pulse durations τ_p and the dead time of the detector τ_d. In these cases, the Carr–Purcell–Meiboom–Gill (CPMG) [1,2] and the Inversion-Recovery (IR) [3] sequences are perfectly adapted to determine T_2, T_1 and the total magnetization, without correction for quantitative analysis. In contrast, in very viscous liquids where $T_1 \gg T_2$, the transversal relaxation time can become so short that the conditions $T_2 \gg \tau_p$ or $T_2 \gg \tau_d$ may not be satisfied. We focus in this paper on these cases and we consider the evolution of the magnetization during the pulses.

The effect of finite pulse duration and relaxation during the pulses has been of concern very early in the development of NMR. In particular in the study

* Corresponding author.
E-mail address: marc.fleury@ifp.fr (M. Fleury).

1631-0748/$ - see front matter © 2007 Académie des sciences. Published by Elsevier Masson SAS. All rights reserved.
doi:10.1016/j.crci.2007.11.004

of chemical exchange [4,5], the relaxation during pulses has important consequences and can be used to select different protons in high-resolution NMR [6]. In this work, we consider low-resolution experiments designed to provide quantitative information about proton species relaxing at different rates to identify their contribution in the system studied. For example, in liquids, we expect to obtain the contribution of high molecular weight components relative to low molecular weight, and for a confined liquid in a porous media, we expect to obtain a precise partitioning of the pore space.

We will first recall the Bloch equations and show that they can be used for the calculation of the magnetization decay during the pulses. Then we present the analytical method to solve the Bloch equations during the pulses as well as the experimental method to observe the effect of pulse duration. The results of the calculation for individual pulses are presented next, along with an experimental validation performed on a FID sequence. Finally we show theoretically and experimentally the effects of relaxation during the pulses on CPMG and IR measurements and propose simple analytical formulae to perform corrections when necessary.

2. Background: Bloch equations and underlying assumptions

Let us consider one set of spins, characterized by:

- a given dipolar interaction correlation time τ_c,
- a given mean square of the dipolar interaction tensor components,

and consequently, by:

- a longitudinal relaxation time T_1;
- a transversal relaxation time T_2.

We will note:

- Oxyz the laboratory frame of reference with Oz along the magnetic induction, B_0;
- OXYz the frame of reference rotating around Oz at the angular frequency $\omega \approx \omega_0 = -\gamma B_0$, where γ is the gyromagnetic factor.

During each sequence the evolution of the magnetization of this spin package is well described by the Bloch equations [7] under the following conditions:

- a homogeneous static magnetic induction, B_0;
- $B_1 \ll B_0$, where B_1 is the amplitude of the magnetic induction $\vec{B_1}$ perpendicular to $\vec{B_0}$, and rotating at the angular frequency ω;
- $<\omega^2>^{1/2}\tau_c < 1$ where $<\omega^2>$ is the second moment of the local dipolar interaction. According to the Bloembergen, Purcell and Pound (BPP) theory [8], this condition is fulfilled if $T_2 > T_{2\text{limit}} \approx 11$ µs for an inter-proton distance $b = 1.78$ Å, which corresponds to the distance between two hydrogen atoms in the methane molecule.

Under these conditions, the effective static induction in the rotating frame OXYz is:

$$\vec{B}_{\text{eff}} = \left(B_0 + \frac{\omega}{\gamma}\right)\vec{k} + \vec{B_1} = \frac{\Delta\omega\vec{k} - \vec{\omega_1}}{\gamma} \tag{1}$$

where $\vec{\omega_1} = -\gamma\vec{B}_1$, $\Delta\omega = \omega - \omega_0$ and $\vec{i}, \vec{j}, \vec{k}$ are the unit vectors of the rotating frame. In this rotating frame, the Bloch equations become:

$$\frac{\mathrm{d}\vec{M}}{\mathrm{d}t} = \gamma\left(\vec{M} \wedge \vec{B_{\text{eff}}}\right) - \frac{M_X\vec{i} + M_Y\vec{j}}{T_2} - \frac{M_z - M_0}{T_1}\vec{k} \tag{2}$$

where M_X, M_Y, M_z are the components of the magnetization $\vec{M}$ in that frame, and M_0, the magnetization at thermal equilibrium along Oz. The use of the Bloch equations during the r.f. pulses is suitable as far as $1/T_{2\rho} = 1/2(1/T_1 + 1/T_2)$ and $1/T_{1\rho} = 1/T_2$, i.e. when $\omega_1\tau_c \ll 1$, where $T_{1\rho}$ and $T_{2\rho}$ are the relaxation times in the rotating frame in the presence of B_1.

3. Analytical and experimental methods

3.1. Resolution of the Bloch equations during a r.f. pulse

Bloch equations were solved during the three different pulses occurring in the CPMG and IR sequences. In each case, the magnetization state before the application of the pulses is linked to the sequences as follows:

- application of a $\pi/2)_X$ pulse when the magnetization is initially along the z axis. This case corresponds to the 90° pulses applied in CPMG, IR and Free Induction Decay (FID) measurements;
- application of a $\pi)_X$ pulse when the magnetization is initially along z. This case corresponds to the inversion pulse in the IR measurement;
- application of a $\pi)_Y$ pulse when the initial magnetization is mainly along Y. This case corresponds to a 180° refocusing pulse in the CPMG sequence.

The analytical resolution was performed for a square pulse (pulse 1 in Fig. 1) and for an "ideal" pulse of zero duration occurring at time $t = 0$ and producing a perfect tilt of the magnetization (pulse 2 in Fig. 1). The analytical calculations, detailed in the Appendix, were performed up to the order ε^2, where $\varepsilon^2 = 1/2\omega_1 T_2$, neglecting the effect of the longitudinal relaxation ($T_1 \gg 2t_p$).

3.2. Experiments

All the experiments have been carried out on a Maran Ultra 23-MHz proton spectrometer from Oxford Instruments. The characteristic time of the free induction decay due to magnetic field inhomogeneities T_2^* is about 1.5 ms. At a constant r.f. amplitude we will note, respectively, τ_p and $2\tau_p$ the $\pi/2$ and π pulse durations. Pulse durations were accurately determined using the standard train90 and train180 pulse sequences. The minimum $\pi/2$ pulse duration is $\tau_{p\,min} = 6$ µs. The dead time (probe + filter) is $\tau_d = 12$ µs.

In order to compare experiments and calculations, we checked that the conditions for applying the Bloch equations are valid:

- the condition $T_2 \ll T_2^*$ is fulfilled and the B_0 induction can be considered homogeneous,
- the condition $B_1 \ll B_0$ because the minimum $\pi/2$ pulse duration is $\tau_{p\,min} = 6$ µs, corresponding to ~42 kHz,
- the relaxation is exponential and not Gaussian.

Viscous hydrocarbon fluids are our main interest, but they usually exhibit a broad distribution of relaxation times [9] and are not suitable for the present study. For the FID and IR tests, we used instead a sample of glycerol at a temperature of −10 °C. At that temperature, we measured T_1 and T_2 values, respectively, of 0.46 ms and 44 ms. For the CPMG tests, we also used glycerol but a temperature of 30 °C ($T_2 = 25$ ms, $T_1 = 43$ ms) and we varied the inter-echo time $TE = 2\tau$ from 100 up to 600 µs. Hence, the ratio $TE/2\tau_p$ varies from 8.3 to 50. In addition, we decreased the number of echoes N_{ech} in order to maintain the ratio τ/N_{ech} constant, i.e. the magnetization decay is recorded over a fixed time interval. In all cases, the zero time origin is at the middle of the first pulse.

4. Results for individual pulses

We present here the results of the calculation for the three pulses used in the IR and CPMG sequences. We note t_p the end of the r.f. pulse with a time origin located at the centre of the pulse, τ_p the duration of a $\pi/2$ pulse (hence $t_p = \tau_p/2$ for a $\pi/2$ pulse and $t_p = \tau_p$ for a π pulse), and M_{X0}, M_{Y0}, M_{z0}, the components of $\vec{M}$ in the rotating frame at time $t = -t_p$. From the values of the magnetization components after the three different pulses (Table 1) under study, we see that there is no difference between the real and ideal pulses for three cases out of nine (Table 1). However, this is true only if one chooses the time origin at the centre of the pulse. For these cases, the considered magnetization component is along the rotation axis. Otherwise, the differences occurring between real and ideal pulses reveal the effect of T_2 relaxation during the pulses. For example, starting from $M_{X0} = 0$, $M_{Y0} = 0$ and $M_{z0} = M_0$ (FID sequence), a residual M_z component remains after the application of a $\pi/2)_X$ pulse (Fig. 2):

$$M_z(t_p) = M_0 \frac{\pi\varepsilon^2}{4} \exp\left(-\frac{\tau_p}{2T_2}\right) \tag{3}$$

Starting from $M_{X0} = M_{Y0} = 0$ and $M_{z0} = M_0$, the effect of relaxation during a $\pi/2)_X$ pulse (duration τ_p) can be obtained from Table 1:

$$\begin{aligned} M_X(t_p) &= 0 \\ M_Y(t_p) &= M_0 \exp\left(-\frac{\tau_p}{2T_2}\right) \\ M_z(t_p) &\approx M_0 \frac{\pi\varepsilon^2}{4} \exp\left(-\frac{\tau_p}{2T_2}\right) \end{aligned} \tag{4}$$

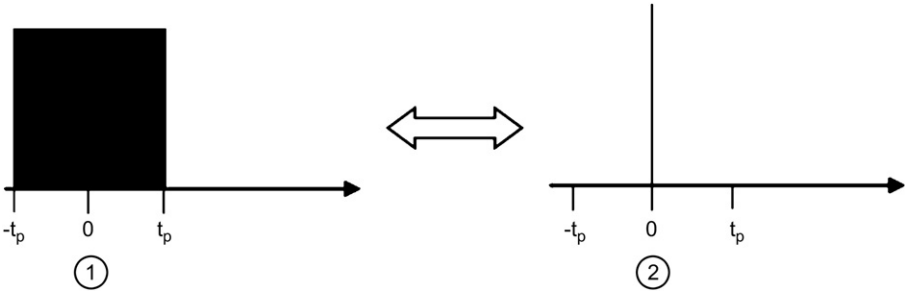

Fig. 1. Real r.f. pulse (1) and ideal r.f. pulse (2).

Table 1
Magnetization components M_X, M_Y, and M_z at the end of $\pi/2)_X$, $\pi)_X$ and $\pi)_Y$ pulses (time t_p) for a real pulse (pulse 1 in Fig. 1) limiting the calculation to ε^2, and an ideal pulse (pulse 2 in Fig. 1), at resonance condition and for $T_2 \ll T_1$

R.f. pulse		M_X (t_p)	M_Y (t_p)	M_z (t_p)
$\pi/2)_X$	1	$M_{X0}\,e^{-\frac{\tau_p}{T_2}}$	$(M_{z0}+\frac{\pi\varepsilon^2}{4}M_{Y0})e^{-\frac{\tau_p}{2T_2}}$	$(-M_{Y0}+\frac{\pi\varepsilon^2}{4}M_{z0})e^{-\frac{\tau_p}{2T_2}}$
	2	$M_{X0}\,e^{-\frac{\tau_p}{T_2}}$	$M_{z0}\,e^{-\frac{\tau_p}{2T_2}}$	$M_{Y0}\,e^{-\frac{\tau_p}{2T_2}}$
$\pi)_X$	1	$M_{X0}\,e^{-\frac{2\tau_p}{T_2}}$	$(-M_{Y0}+\frac{\pi\varepsilon^2}{2}M_{z0})e^{-\frac{\tau_p}{T_2}}$	$(-M_{z0}-\frac{\pi\varepsilon^2}{2}M_{Y0})e^{-\frac{\tau_p}{T_2}}$
	2	$M_{X0}\,e^{-\frac{2\tau_p}{T_2}}$	$-M_{Y0}\,e^{-\frac{\tau_p}{T_2}}$	$-M_{z0}\,e^{-\frac{\tau_p}{T_2}}$
$\pi)_Y$	1	$(-M_{X0}-\frac{\pi\varepsilon^2}{2}M_{z0})e^{-\frac{\tau_p}{T_2}}$	$M_{Y0}\,e^{-\frac{2\tau_p}{T_2}}$	$(-M_{z0}+\frac{\pi\varepsilon^2}{2}M_{X0})e^{-\frac{\tau_p}{T_2}}$
	2	$-M_{X0}\,e^{-\frac{\tau_p}{T_2}}$	$M_{Y0}\,e^{-\frac{2\tau_p}{T_2}}$	$-M_{z0}\,e^{-\frac{\tau_p}{T_2}}$

M_{X0}, M_{Y0}, and M_{z0} are the magnetization components at the beginning of the pulse at time $-t_p$; τ_p is the duration of a $\pi/2$ pulse.

As already mentioned, the magnetization is not perfectly tilted along OY and the effective tilt angle is less than 90°. Considering the measurable component M_Y, there is an attenuation due to the decrease of the overall magnetization modulus, and to the imperfect tilt angle. We define the attenuation $\mathrm{Att}_{\pi/2}$ of the M_Y component after a $\pi/2)_X$ pulse as:

$$\mathrm{Att}_{\pi/2}(t_p)=\frac{M_Y(t_p)}{M_0}\approx\exp\left(-\frac{\tau_p}{2T_2}\right) \tag{5}$$

Starting from $M_{X0}=M_{Y0}=0$ and $M_{z0}=M_0$, the effect of relaxation during a $\pi)_X$ pulse (pulse duration $2\tau_p$) can be obtained from Table 1:

$$\begin{aligned} M_X(t_p)&=0\\ M_Y(t_p)&\approx M_0\frac{\pi\varepsilon^2}{2}\exp\left(-\frac{\tau_p}{T_2}\right)\\ M_z(t_p)&=-M_0\exp\left(-\frac{\tau_p}{T_2}\right)\end{aligned} \tag{6}$$

In this case, the effective tilt angle is 180°, the remaining magnetization along Y is negligible, and there is an attenuation of the magnetization amplitude. Similarly, we define the attenuation of the M_z component after a $\pi)_X$ pulse as:

$$\mathrm{Att}_{\pi}(t_p)=\frac{M_z(t_p)}{-M_0}\approx\exp\left(-\frac{\tau_p}{T_2}\right) \tag{7}$$

Finally, whatever the magnetization components M_{X0}, M_{Y0} and M_{z0} may be, the effect of relaxation during a $\pi)_Y$ pulse (pulse duration $2\tau_p$) can be obtained from Table 1:

$$M_Y(t_p)=M_{Y0}\exp\left(-\frac{2\tau_p}{T_2}\right) \tag{8}$$

It is obvious that when rotating around the Y axis during the pulse, the M_Y component relaxes exponentially with a time constant T_2.

In practical situation, the detection of the magnetization is only possible after a dead time τ_d which is typically of the order of 10 µs. The resulting attenuation is then expressed as:

$$\mathrm{Att}_{\mathrm{dead}}=\exp\left(-\frac{\tau_d}{T_2}\right) \tag{9}$$

and the magnetization is then given by (in the case of a $\pi/2$ pulse):

$$M_Y(t_p+\tau_d)\approx M_0\mathrm{Att}_{\pi/2}(t_p)\mathrm{Att}_{\mathrm{dead}} \tag{10}$$

To test experimentally Eq. (10), we used glycerol relaxing at $T_2=460$ µs at −10 °C and we varied the $\pi/2$ pulse duration τ_p from 6.2 µs up to 380 µs. Therefore, the τ_p/T_2 ratio varies from 0.01 to 0.83. There is a good agreement between experimental data (first FID points) and the total predicted attenuation $\mathrm{Att}_{\pi/2}$ $\mathrm{Att}_{\mathrm{dead}}$ (Fig. 3). Note that this curve does not reach 1 for small values of τ_p/T_2. Indeed, we varied the pulse duration τ_p and not the T_2 value, so that there is a constant attenuation factor $\mathrm{Att}_{\mathrm{dead}}$, corresponding to:

$$\mathrm{Att}_{\mathrm{dead}}=\exp\left(-\frac{\tau_d}{T_2}\right)=\exp\left(-\frac{12}{460}\right)\approx 0.97 \tag{11}$$

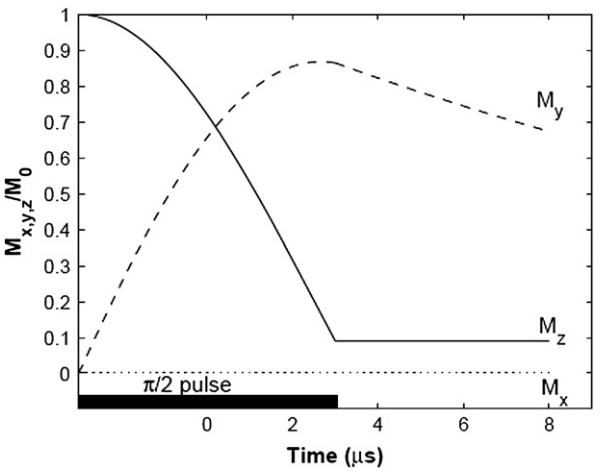

Fig. 2. Calculation of M_X, M_Y, and M_z as a function of time during and after a $\pi/2)_X$ pulse for $\tau_p=6$ µs, $T_1=10$ s and $T_2=20$ µs.

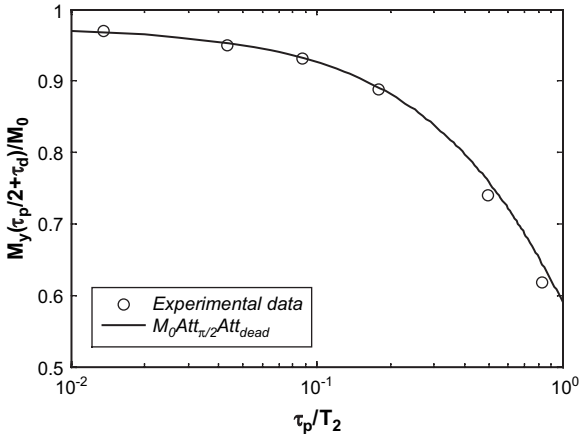

Fig. 3. Amplitude of the first measurable point of the FID versus τ_p/T_2 for a glycerol sample at −10 °C; the spectrometer dead time $\tau_d = 12$ μs is taken into account in the analytic formula, see Eq. (10).

5. Results for the IR sequence

We treat here the Inversion-Recovery (IR) pulse sequence commonly used for T_1 measurements and described in Fig. 4. We can calculate the magnetization components during this sequence using the results obtained for individual pulses (Table 1).

At $t_0 = -\tau_p$, the magnetization is along z, therefore:

$$\begin{aligned} M_X(t_0) &= 0 \\ M_Y(t_0) &= 0 \\ M_z(t_0) &= M_0 \end{aligned} \tag{12}$$

After the $\pi)_X$ pulse, at $t_1 = \tau_p$ the magnetization components are:

$$\begin{aligned} M_X(t_1) &= 0 \\ M_Y(t_1) &\approx M_0 \frac{\pi\varepsilon^2}{2} \exp\left(-\frac{\tau_p}{T_2}\right) \\ M_z(t_1) &= -M_0 \exp\left(-\frac{\tau_p}{T_2}\right) \end{aligned} \tag{13}$$

Then, the magnetization components relax exponentially, M_X and M_Y decreasing with a time constant T_2 and M_z with a time constant T_1, during the time d_1. So, at time $t_2 = \tau_p + d_1$ the magnetization components can be written as:

$$\begin{aligned} M_X(t_2) &= 0 \\ M_Y(t_2) &\approx M_0 \frac{\pi\varepsilon^2}{2} \exp\left(-\frac{\tau_p}{T_2}\right) \exp\left(-\frac{d_1}{T_2}\right) \\ M_z(t_2) &= M_0 + \left(-M_0 \exp\left(-\frac{\tau_p}{T_2}\right) - M_0\right) \exp\left(-\frac{d_1}{T_1}\right) \end{aligned} \tag{14}$$

After the $\pi/2)_x$ pulse, at time $t_3 = \tau_p + d_1 + \tau_p$, the magnetization components are:

$$\begin{aligned} M_X(t_3) &= 0 \\ M_Y(t_3) &\approx \left[M_0 - \left(M_0 \exp\left(-\frac{\tau_p}{T_2}\right) + M_0\right) \exp\left(-\frac{d_1}{T_1}\right) + M_0 \frac{\pi\varepsilon^2}{4} \frac{\pi\varepsilon^2}{2} \exp\left(-\frac{\tau_p}{T_2}\right) \exp\left(-\frac{d_1}{T_2}\right)\right] \exp\left(-\frac{\tau_p}{2T_2}\right) \\ M_z(t_3) &\approx \left[\frac{\pi\varepsilon^2}{2} M_0 \exp\left(-\frac{\tau_p}{T_2}\right) \exp\left(-\frac{d_1}{T_2}\right) + \frac{\pi\varepsilon^2}{2}\left(M_0 + \left(M_0 \exp\left(-\frac{\tau_p}{T_2}\right) - M_0\right) \exp\left(-\frac{d_1}{T_1}\right)\right)\right] \exp\left(-\frac{\tau_p}{2T_2}\right) \end{aligned} \tag{15}$$

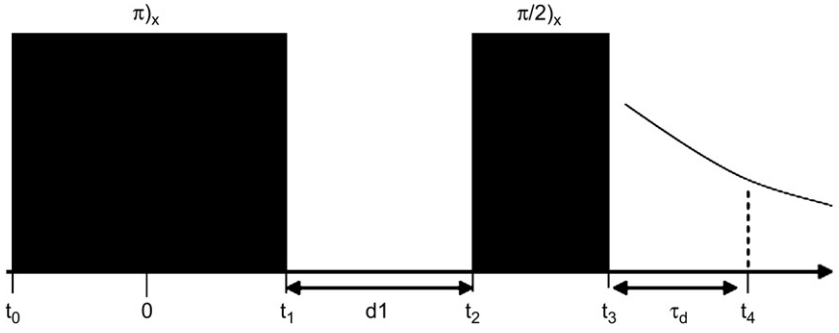

Fig. 4. Inversion-Recovery pulse sequence.

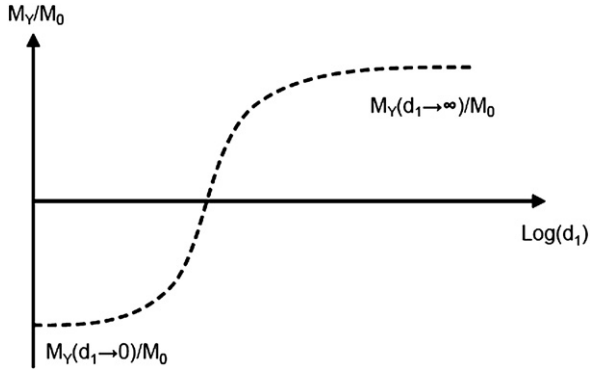

Fig. 5. Typical Inversion-Recovery curve.

After a dead time τ_d, neglecting terms of order ε^4 in Eq. (15), the detected M_Y component at time $t_4 = \tau_p + d_1 + \tau_p + \tau_d$ can be written as:

$$M_Y(t_4) = \left[M_0 - \left(M_0 \exp\left(-\frac{\tau_p}{T_2}\right) + M_0\right) \times \exp\left(-\frac{d_1}{T_1}\right)\right] \exp\left(-\frac{\tau_p}{2T_2}\right) \exp\left(-\frac{\tau_d}{T_2}\right) \quad (16)$$

As a consequence, even if the T_1 measurement is affected by transversal relaxation during the pulses, the M_Y component relaxes exponentially when d_1 is varied. A typical Inversion-Recovery curve is shown in Fig. 5. Using Eq. (16), we can write the expressions of M_Y (t_4, $d_1 \to 0$) and M_Y (t_4, $d_1 \to \infty$) as follows:

$$M_Y(t_4, d_1 \to 0) = -M_0 \exp\left(-\frac{\tau_p}{T_2}\right) \exp\left(-\frac{\tau_p}{2T_2}\right) \times \exp\left(-\frac{\tau_d}{T_2}\right) \quad (17)$$

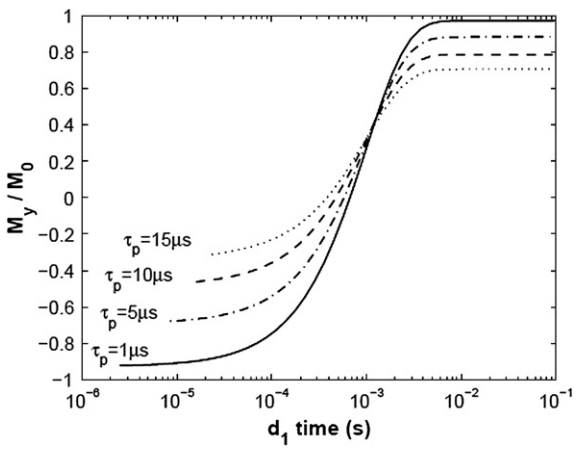

Fig. 6. Calculated Inversion-Recovery curves for different pulse durations with $\tau_d = 0$, $T_1 = 1$ ms and $T_2 = 20$ µs.

$$M_Y(t_4, d_1 \to \infty) = M_0 \exp\left(-\frac{\tau_p}{2T_2}\right) \exp\left(-\frac{\tau_d}{T_2}\right) \quad (18)$$

Thus, using the expressions of the attenuations defined in Eqs. (5), (7) and (9), one can write these expressions as:

$$M_Y(t_4, d_1 \to 0) = -M_0 \mathrm{Att}_\pi(\tau_p) \mathrm{Att}_{\pi/2}(\tau_p/2) \mathrm{Att}_{dead} \quad (19)$$

$$M_Y(t_4, d_1 \to \infty) = M_0 \mathrm{Att}_{\pi/2}(\tau_p/2) \mathrm{Att}_{dead} \quad (20)$$

The common way to treat the IR curves is to apply the following transform:

$$T(d_1) = M_Y(d_1 \to \infty)\left(1 - \frac{M_Y(d_1)}{M_Y(d_1 \to \infty)}\right) \quad (21)$$

yielding a curve decreasing from $M_Y(d_1 \to \infty) - M_Y(d_1 \to 0)$ to zero. This curve is then treated as an exponential decay. In consequence, the magnetization amplitude of a T_1 component can be defined as $M_Y(d_1 \to \infty) - M_Y(d_1 \to 0)$, rather than the classically expected amplitude $2M_0$ obtained when $T_2 \gg \tau_p$ and τ_d. The amplitude ratio Att_{IR} is:

$$\mathrm{Att}_{IR} = \frac{M_Y(d_1 \to \infty) - M_Y(d_1 \to 0)}{2M_0} \quad (22)$$

Using Eqs. (19) and (20), one can write this amplitude ratio as:

$$\mathrm{Att}_{IR} = \frac{\left[1 + \mathrm{Att}_\pi(\tau_p)\right] \mathrm{Att}_{\pi/2}(\tau_p/2) \mathrm{Att}_{dead}}{2} \quad (23)$$

The full IR sequence has been calculated for different values of τ_p (Fig. 6). The dead time has been set to zero for simplicity.

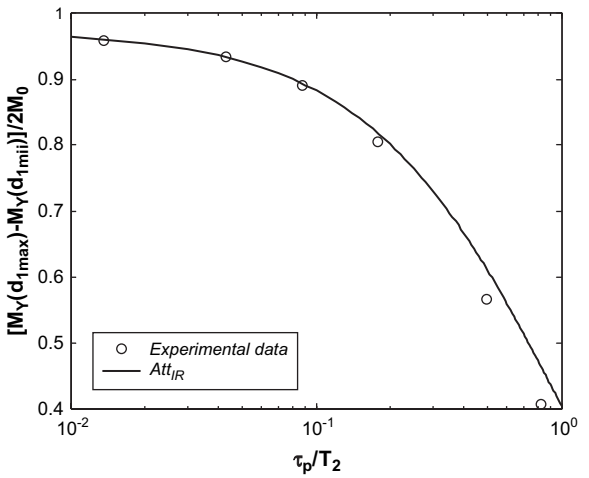

Fig. 7. Total amplitude from IR measurements versus τ_p/T_2, glycerol sample at −10 °C; a dead time τ_d of 12 µs is taken into account in the analytic formula given in Eq. (23).

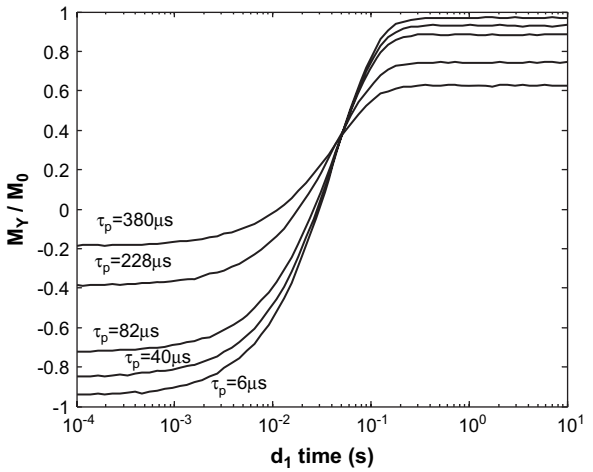

Fig. 8. IR measurements for a glycerol sample at −10 °C for different values of pulse duration at resonance condition; the same relaxation time is obtained for all curves ($T_1 = 46$ ms).

As a result of Eqs. (19) and (20), $M_Y(d_1 \to 0)$ is more attenuated than $M_Y(d_1 \to \infty)$, yielding non-symmetric curves, as presented in Fig. 6. However, despite this asymmetry, the relaxation time T_1 is constant, as predicted by Eq. (16).

In order to obtain an experimental verification of Eq. (23), T_1 measurements were performed for different pulse durations τ_p on a glycerol sample at −10 °C ($T_2 = 460$ µs). The detected amplitude $[M_Y\ (d_{1\max}) - M_Y(d_{1\min})]/2M_0$ with $d_{1\max} = 10$ s and $d_{1\min} = 10$ µs as a function of τ_p/T_2 is in agreement (Fig. 7) with the analytical attenuation $\mathrm{Att_{IR}}$ given by Eq. (23). For each IR measurement (Fig. 8), non-symmetric curves are measured, as predicted, but the same T_1 value (46 ms) is deduced independently of the pulse duration.

6. Results for the CPMG sequence

We have already studied separately the effect of the pulses used in a CPMG measurement (Table 1). If we consider the pulse sequence described in Fig. 9, we can calculate the magnetization components during the sequence. At $t_0 = -\tau_p/2$, the magnetization is along Oz, therefore:

$$\begin{aligned} M_X(t_0) &= 0 \\ M_Y(t_0) &= 0 \\ M_z(t_0) &= M_0 \end{aligned} \tag{24}$$

After the $\pi/2)_X$ pulse, at $t_1 = \tau_p/2$, the magnetization components are:

$$\begin{aligned} M_X(t_1) &= 0 \\ M_Y(t_1) &= M_0 \exp\left(-\frac{\tau_p}{2T_2}\right) \\ M_z(t_1) &\approx M_0 \frac{\pi\varepsilon^2}{4} \exp\left(-\frac{\tau_p}{2T_2}\right) \end{aligned} \tag{25}$$

Then the M_Y component relaxes exponentially without any effect of the $\pi)_Y$ pulses during a time $2\tau - t$. So at $t = 2\tau$, the M_Y component can be written as:

$$\begin{aligned} M_Y(2\tau) &= M_0 \exp\left(-\frac{\tau_p}{2T_2}\right) \exp\left(-\frac{2\tau - t_1}{T_2}\right) \\ &= M_0 \exp\left(-\frac{2\tau}{T_2}\right) \end{aligned} \tag{26}$$

As a consequence, if the time origin is taken at the middle of the first pulse, relaxation during the pulses does not affect the results of the CPMG measurement.

We have calculated the full sequence by Bloch equations, resolution for an extreme case, where T_2 ($= 40$ µs) $\ll T_1$ ($= 10$ s) and $\tau_p = 20$ µs. We simulated three echoes with a half inter-echo time $\tau = 30$ µs (Fig. 10).

We also tested the analytical result of Eq. (26) experimentally. Several CPMG measurements were performed on a glycerol sample at 30 °C ($T_2 = 44$ ms), as described in a previous section. The measured magnetization decays were fitted using a single exponential

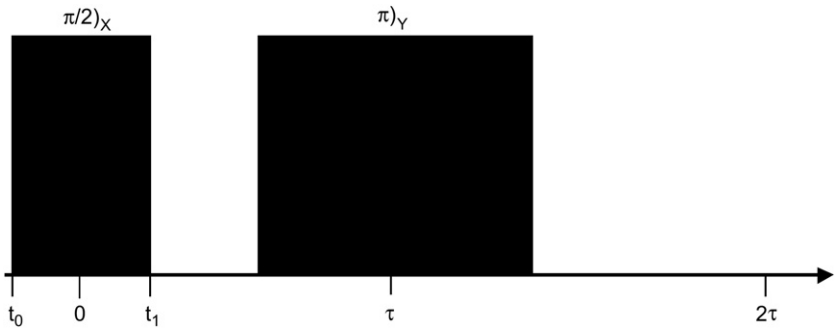

Fig. 9. CPMG pulse sequence considered in this work.

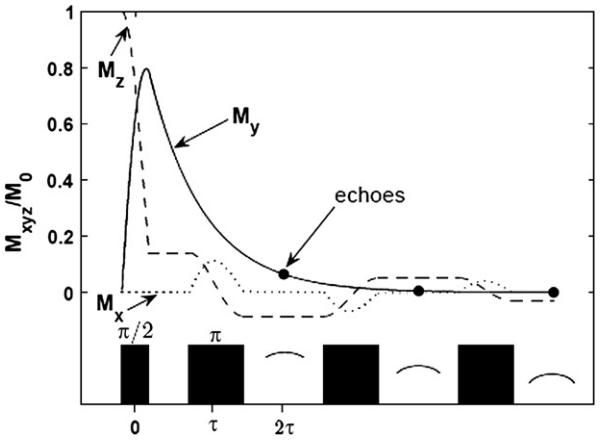

Fig. 10. Magnetization (M_X, M_Y, M_z) versus time during a CPMG sequence (3 echoes with $\tau = 30$ ms, $\pi/2$ pulse length $\tau_p = 20$ μs, $T_1 = 10$ s and $T_2 = 40$ μs).

component and each experiment led to the same T_2 value whatever the τ value or the number of echoes or the total π pulse duration in the CPMG sequence. This is true if the magnetization is recorded as a function of time counted from the middle of the first pulse, in particular for long π pulse. A simple fitting procedure using the data points at time $t = 2n\tau$ ($n = 1, 2\ldots$) yields the total magnetization M_0 and T_2. According to these results, we conclude that the CPMG sequence has theoretically the ability to detect both the amplitude and time constant for very short T_2 values. However, when a distribution of relaxation time is present in the fluid (as often encountered), the shortest components are described only by a few echoes. Therefore, in a multi-exponential fitting, the weight of the longest components is much larger, yielding a poor determination of the short components.

7. Conclusion

The calculations presented in this article treat the problem of short T_2 relaxation time detection. The transversal relaxation during the pulses has been calculated by analytical resolution of Bloch equations. The remarkable agreement observed between experimental and theoretical attenuations establishes the adequacy of these equations to solve the specific problem of relaxation during the pulses. Although the description of the attenuation using simple exponential functions is not exact, it is sufficient to represent experimental results.

The main conclusions concerning relaxation time measurements are as follows:

- for the FID sequence, relaxation during the pulse yields underestimated magnetization values. This magnetization loss is predicted by Eq. (10), in good agreement with experimental data;
- for the CPMG sequence, we have shown that there is no effect of relaxation during the pulses. Neither the number nor the duration of the pulses will affect the determination of the relaxation time T_2;
- for the IR sequence, transversal relaxation during pulses and dead time yields a non-negligible underestimation of magnetization and asymmetric IR curves. This magnetization loss is predicted by Eq. (23), in good agreement with experimental data. However, the T_1 value deduced from IR curves is not affected by the asymmetry.

Appendix. Analytical resolution of the Bloch equations during a r.f. pulse

We analyse the effect of a r.f. pulse during a time interval $[-t_p; t_p]$, neglecting the effect of the longitudinal relaxation ($T_2 \ll T_1$). We note $\vec{\omega}_1 = -\gamma\vec{B}_1$, τ_p, the $\pi/2$ r.f. pulse duration, and M_{X0}, M_{Y0}, M_{z0}, the components of $\vec{M}$ in the rotating frame at time $t = -t_p$. Let us consider two typical cases.

- Case 1: when $\vec{B_1}$ is applied along OX in the rotating frame. Bloch equations become:

$$\frac{dM_X}{dt} = -\frac{M_X}{T_2};\ \frac{dM_Y}{dt} = -\frac{M_Y}{T_2} - \omega_1 M_z;\ \frac{dM_z}{dt} = \omega_1 M_Y \tag{A1}$$

If $\varepsilon^2 = 1/2\omega_1 T_2 \leq 1$, for $-t_p < t < t_p$, the solution is:

$$\begin{aligned} M_X(t) &= M_{X0}\exp\left(-\frac{t+t_p}{T_2}\right) \\ M_Y(t) &= \exp\left(-\frac{t+t_p}{2T_2}\right)\left(M_{Y0}\cos q\left(t+t_p\right)\right. \\ &\quad \left. + M_{z0}\sin q\left(t+t_p\right)\right) \\ M_z(t) &= \exp\left(-\frac{t+t_p}{2T_2}\right)\left(M_{z0}\cos q\left(t+t_p\right)\right. \\ &\quad \left. - M_{Y0}\sin q\left(t+t_p\right)\right) \end{aligned} \tag{A2}$$

with $q = \omega_1\sqrt{1-\varepsilon^2}$.

- Case 2: when $\vec{B_1}$ is applied along OY in the rotating frame. Bloch equations become:

$$\frac{dM_X}{dt} = -\frac{M_X}{T_2} + \omega_1 M_z;\ \frac{dM_Y}{dt} = -\frac{M_Y}{T_2};\ \frac{dM_z}{dt} = -\omega_1 M_X \tag{A3}$$

If $\varepsilon^2 = 1/2\omega_1 T_2 \leq 1$, for $-t_p < t < +t_p$, the solution is:

$$\begin{aligned} M_X(t) &= \exp\left(-\frac{t+t_p}{2T_2}\right)\left(M_{Y0}\cos q(t+t_p)\right. \\ &\quad \left. -M_{z0}\sin q(t+t_p)\right) \\ M_Y(t) &= M_{X0}\exp\left(-\frac{t+t_p}{T_2}\right) \\ M_z(t) &= \exp\left(-\frac{t+t_p}{2T_2}\right)\left(M_{z0}\cos q(t+t_p)\right. \\ &\quad \left. + M_{Y0}\sin q(t+t_p)\right) \end{aligned} \tag{A4}$$

Next, we will consider the case where $\varepsilon \ll 1$, corresponding to the operating range of the NMR technique, so that we limit the development of sin qt and cos qt up to ε^2 in Eqs. A2 and A4. The components of $\vec{M}$ obtained at t_p are defined:

- after a $\pi/2)_X$ r.f. pulse, corresponding to $t_p = \tau_p/2$, by:

$$\begin{aligned} M_X(t_p) &= M_{X0}\exp\left(-\frac{\tau_p}{T_2}\right) \\ M_Y(t_p) &= \exp\left(-\frac{\tau_p}{2T_2}\right)\left(\frac{\pi\varepsilon^2}{4}M_{Y0} + M_{z0}\right) \\ M_z(t_p) &= \exp\left(-\frac{\tau_p}{2T_2}\right)\left(\frac{\pi\varepsilon^2}{4}M_{z0} - M_{Y0}\right) \end{aligned} \tag{A5}$$

- after a $\pi)_X$ r.f. pulse, corresponding to $t_p = \tau_p$, by

$$\begin{aligned} M_X(t_p) &= M_{X0}\exp\left(-\frac{2\tau_p}{T_2}\right) \\ M_Y(t_p) &= \exp\left(-\frac{\tau_p}{T_2}\right)\left(-M_{Y0} + \frac{\pi\varepsilon^2}{2}M_{z0}\right) \\ M_z(t_p) &= \exp\left(-\frac{\tau_p}{T_2}\right)\left(-M_{z0} - \frac{\pi\varepsilon^2}{2}M_{Y0}\right) \end{aligned} \tag{A6}$$

- after a $\pi)_Y$ r.f. pulse, corresponding to $t_p = \tau_p$,

$$\begin{aligned} M_X(t_p) &= \exp\left(-\frac{\tau_p}{T_2}\right)\left(-M_{X0} - \frac{\pi\varepsilon^2}{2}M_{z0}\right) \\ M_Y(t_p) &= M_{Y0}\exp\left(-\frac{2\tau_p}{T_2}\right) \\ M_z(t_p) &= \exp\left(-\frac{\tau_p}{T_2}\right)\left(-M_{z0} + \frac{\pi\varepsilon^2}{2}M_{X0}\right) \end{aligned} \tag{A7}$$

References

[1] H. Carr, E. Purcell, Phys. Rev. 94 (1954) 630.
[2] S. Meiboom, D. Gill, Rev. Sci. Instrum. 29 (1958) 688.
[3] R. Vold, J. Waugh, M. Klein, D. Phelps, J. Chem. Phys. 48 (8) (1968) 3831.
[4] C.S. Johnson, M. Saunders, J. Chem. Phys. 43 (1965) 4170.
[5] D. Lankhorst, J. Schriever, J.C. Leyte, J. Magn. Reson. 51 (1983) 430.
[6] R. Freeman, S. Wittekoek, J. Magn. Reson. 1 (1969) 238.
[7] F. Bloch, Phys. Rev. 70 (1946) 460.
[8] N. Bloembergen, E. Purcell, R. Pound, Phys. Rev. 73 (1948) 679.
[9] K.J. Dunn, D.J. Bergman, G.A. La Torraca, Nuclear Magnetic Resonance, Petrophysical and Logging applications, in: Seismic Exploration, vol. 32, Pergamon, 2002.